

#### **TNO PUBLIC**

**TNO** report

TNO2021 R11603 | Final report

Turbulence intensity calculation using Gaussian Processes on the wind speeds measured by nacelle mounted lidar Westerduinweg 3 1755 LE Petten P.O. Box 15 1755 ZG Petten The Netherlands

www.tno.nl

T +31 88 866 50 65

Date 15 October 2021

Author(s) C. Liu; E.J. Rose

Copy no No. of copies

Number of pages

19 (incl. appendices)

Number of appendices

Sponsor RVO - TKI Wind op Zee HER

Project name GE Haliade X Demonstration: Innovations in Type Certification

Project number 060.34375

#### All rights reserved.

No part of this publication may be reproduced and/or published by print, photoprint, microfilm or any other means without the previous written consent of TNO.

In case this report was drafted on instructions, the rights and obligations of contracting parties are subject to either the General Terms and Conditions for commissions to TNO, or the relevant agreement concluded between the contracting parties. Submitting the report for inspection to parties who have a direct interest is permitted.

© 2021 TNO

## Summary

Wind measurement is probably the most essential input for any wind energy technology applications. The wind speed and turbulence intensity are traditionally and still popularly measured with cup anemometer or sonic anemometer.

In recent years lidar technology, and particularly nacelle lidar technology, emerged in the wind energy industry with its many advantages: reduced cost compared to meteorological mast; always measuring in front of the wind turbine to enable a wider measurement sector with high correlation to wind power; measuring at more ranges; measuring over a plane or volume instead of a point; potability; assisting smart wind turbine control etc. It is adopted by the industry through various pilot and commercial projects over the world for warranty Power Performance Testing already. The IEC standards based on the best practices for ground based lidar, nacelle mounted lidar and floating lidar are coming on their way. However lidar is still not accepted for turbulence measurements.

A novel application of Machine Learning for lidar measurement was developed by TNO Wind Energy, based on Gaussian Process regression, to produce reconstructed wind field from lidar measurements. In this report, the potentials of using Gaussian Process regression to improve the wind turbulence intensity for lidar wind measurements are studied with several Gaussian Process implementation tests: upsampling the data to higher frequency, filling missing data, predicting in space and predicting in the center of the beams. For a two-beam lidar, although the Gaussian Process does not show effective improvements for calculating turbulence intensity. The main reasons are firstly that its bias towards the mean values when predicting away from measurement data, and secondly that it relies on the methods of converting the radial wind speeds to horizontal wind speeds. However the results do demonstrate that Gaussian Process can be applied to almost any lidar system to predict beam radial wind speeds in space and time. And there is still potential to improve turbulence intensity by using lidar with more beams for predictions within a volume as opposed to a plane, or by further developing Gaussian Process mechanisms to calculate turbulence intensity with different methods.

TNO acknowledges Leosphere for using their lidar data in this project.

# Contents

	Summary	2
1	Introduction	4
2	Technical Background	5
2.1	Wind turbine Type Certification (TC)	5
2.2	Lidar	5
2.3	Gaussian Process (GP)	6
3	Turbulence Intensity calculation	8
3.1	Wind dataset	8
3.2	Wind field reconstruction	10
3.3	GP implementation	
3.4	Results	11
4	Conclusions	18
5	References	19

## 1 Introduction

Wind measurement is probably the most top essential input for any wind energy technology applications. The wind speed and turbulence intensity (TI) are traditionally and still popularly measured with cup anemometer or sonic anemometer.

In recent years the lidar (Light Detection and Ranging) technology, and particularly nacelle lidar technology, emerged in the wind energy industry with its many advantages: reduced cost compared to meteorological mast (MM); always measuring in front of the wind turbine to enable a wider measurement sector with high correlation to wind power; measuring at more ranges; measuring over a plane or volume instead of a point; potability; assisting smart wind turbine control etc. It is adopted by the industry through various pilot and commercial projects over the world for Power Performance Testing already. The IEC standards based on the current best practices for ground based lidar, nacelle mounted lidar and floating lidar are coming on their way. However lidar is still not accepted for turbulence measurements [1].

A novel application of Machine Learning (ML) for lidar measurement was developed by TNO Wind Energy [4], based on Gaussian Process (GP) regression, to produce reconstructed wind fields from lidar measurements. In this report, the potential of using GP regression to improve the wind TI calculation for lidar wind measurements are studied and the results are presented.

Chapter 2 describes the technical background about wind turbine Type Certification (TC), lidar and GP. Chapter 3 describes the wind field reconstruction using GP and results from different implementations tests. Chapter 4 gives the conclusions and recommendations for future work.

## 2 Technical Background

### 2.1 Wind turbine Type Certification (TC)

Wind turbine TC is a must-have for wind turbine OEMs to be able to bring their products to market. The type certification process provides confirmation that the wind turbine type, components and systems have been designed, manufactured and tested in conformity with the requirements as mandated by international standards and site-specific condition. It is an all-inclusive verification of wind turbine safety, reliability and performance according to standards, which makes it quite a time consuming process. Moreover with the increase of wind turbine size, the time of the type certification process is also increasing.

Type testing evaluation is part of the type certification, where a prototype is erected and tested on site. During type testing, the wind properties need to be measured. Following the latest IEC standard [2], a remote sensing device (RSD) can be deployed, but this is limited to non-complex terrain and a short MM (not less than the minimum of the wind turbine lower blade tip-height or 40m) must exist for comparison purpose.

Lidar has been in the spotlight of IEC standardisation over the recent years. It is not only because of its high potentials to bring down both the time and cost of wind measurement, but also because of the innovative applications of lidar which can reduce the Cost of Energy (CoE) effectively such as yaw misalignment correction, site suitability pre-construction studies and lidar assisted control etc. The draft IEC guideline IEC 61400-50-2 for application of ground based lidar (GBL) and the draft IEC guideline IEC 61400-50-3 for application of nacelle mounted lidar (NML) are submitted to all IEC members in 2021 and on the way to the final release. The IEC guideline IEC 61400-50-4 for application of floating lidar will also come as planned in 2022. It will be a big step to have all those IEC standards to speed up the application of lidar for TC, however there are still many research challenges for further applications of lidar, such as the application in complex terrain or superseding MM completely.

## 2.2 Lidar

Lidar is based on Doppler shift of the backscattered light to determine the wind speed in the line of sight (LOS) direction.

There are different types of lidar. Most commercial wind lidars use homodyne detection to determine the Doppler shift. With homodyne detection information on the magnitude of the shift is gathered, but no information on whether it is positive or negative which means the wind is towards the lidar or away from the lidar is unknown. The heterodyne detection gathers both magnitude and sign but requires more hardware which drives up the cost to produce a lidar. Another way to categorize the lidar is based on it is light source: pulsed wave or continuous wave. For pulsed lidar, the time of the pulsed light used to travel to the target and back is used to determine the measurement distance. For continuous wave lidar, the measurement distance is determined by focus. According to the application, the lidar is also commonly categorized as GBL, NML, scanning lidar and floating lidar.

The application of different lidar technology in wind energy industry had been researched for many years. TNO Wind Energy (formerly known as ECN Wind Energy) also conducted a large test campaign to study and quantify numerous advantages of GBL, NML and scanning lidar [3].

Nowadays lidar is accepted and used for warranty Power Performance Testing (PPT). However for TC, an installed lidar without accompanying MM is still not accepted in the latest IEC standard [2] to provide wind measurements for power performance and mechanical loads measurements. One of the possible reasons is that current lidar technology obtains TI measurements differently than a wind cup anemometer or sonic anemometer mounted on a MM.

Lidar technologies perform averaging over a large measurement volume (i.e. the probe volume). For turbulence measurements, this has a similar effect as applying a low pass filter, which reduces the standard deviation of the measured signal (i.e. wind velocities) resulting in reduced values of the TI. Deducing unfiltered turbulence statistics from the raw lidar data has been and remains the most challenging aspect of lidar application and many research has been done to develop algorithms to improve this situation [1].

Another drawback of lidar technology is that using a single lidar with only LOS wind speeds makes it impossible to distinguish between wind shear and wind direction. This is called the cyclops dilemma (ref?). Currently the standard wind field reconstruction algorithms from lidar manufacturers assume homogeneous wind flow.

## 2.3 Gaussian Process (GP)

As described in [4], TNO wind energy has developed a novel ML algorithm based on GP regression to remove the assumptions when producing 3D wind fields from lidar measurements. This algorithm is naturally robust to overfitting and predicts uncertainty in the prediction derived from data density and machine error. In a GP, it is assumed that variables in a stochastic process are jointly normally distributed, and can be described as such. A GP is fully specified by a mean and a covariance function, and can be fitted to any variable as illustrated in Figure 1. These properties allow the machine learning algorithm to predict anywhere in the input space and time, essentially turning it into a powerful regression tool. As such, GP provides a number of powerful benefits:

- prediction of higher-frequency data,
- interpolation of missing data,
- spatial prediction of data within the measurement volume and
- calculation of prediction uncertainty is included in the process itself.

The main limitation of GP are its bias towards the mean when predicting away from measurement data.

An additional limitation to the overall methodology is in regards to how the GP is used. They predict radial wind speeds, and so conversion to horizontal wind speed (HWS) is highly dependent on the methodology used.

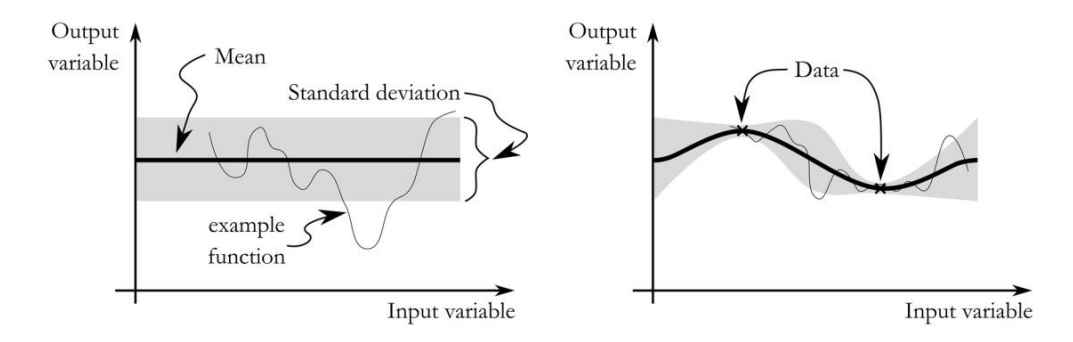


Figure 1 Basic overview of Gaussian Processes: left, prior; right, posterior [4]

## 3 Turbulence Intensity calculation

TNO has been working with different types of lidar, including GBL and scanning lidar configurations. While HWS is resolved well by lidar systems, TI continues to be a challenge topic. Specifically, the TI measured by lidar is not as the same as that measured by a cup or sonic anemometer due to volume-averaging (as mentioned in 2.2). In this report, a two-beam NML is considered to apply the GP. The purpose of the works is to assess the ability for a GP to improve TI measurement from a NML.

The following goals are considered:

- apply the GP to a two-beam NML, producing wind statistics,
- analyse the effect of the GP on lidar-based TI predictions, and
- explore potential ways to improve the TI calculations, using the GP.

#### 3.1 Wind dataset

The dataset used for this campaign is that for the Lawine campaign [5]. The details of this campaign, including information on the installation, can be found in the instrumentation report [6]. A two-beam Wind Iris lidar was installed on a turbine in order to investigate turbine performance. The flat terrain and proximity to a MM makes this an ideal dataset to test the GP on.

An 8-hour analysis period was chosen when the wind was aligned in the direction from the mast to the turbine, unobstructed, at high wind speeds (above 10 m/s). During this period, the lidar was also configured to measure at a distance equal to that between the turbine and the mast. If the turbine was pointing 15° offset from the mast direction, one of the two lidar beams would be measuring at the MM location. As such, filters on the data were:

- Measurement sector: During the 8-hour period, the wind was consistent, flowing from the south-west, ensuring it passed the MM prior to reaching the wind turbine.
   As such, with the lidar mounted on the turbine, it would always point close to the MM within the period.
- Wind speed: The period analyzed had wind speeds above the rated wind speed
  of the mounted turbine, ensuring the lidar would be facing the correct direction.
  Specifically, ten-minute averaged HWS from the MM was never recorded as
  lower than 10 m/s.
- lidar status: The lidar itself must be outputting an operational status for all ranges so the signals in Table 1 should be available.
- CNR Value: The CNR was bounded by -22 dB on the lower end and -3 dB on the
  upper end. High values of the CNR values indicate obstruction of the lidar beam
  (such as by the MM itself), while low values indicate atmospheric events, which
  can affect results.

Table 1 below shows the measured signals from the WindIris lidar, while Table 2 shows the same used from the met mast. Table 3 provides a list and description of all outputs from the WindIris lidar.

Table 1 Measured signals WindIris

Measured signals WindIris						
		Sampling				
Description	Short name	rate [Hz.]	Unit			
Tilt	T6_WI_tilt	1	0			
Roll	T6_WI_roll	1	0			
	Short name xx = 1 (80m), 2 (120m), 3 (160m), 4 (200m), 5 (240m), 6 (280m), 7					
Description	(320m), 8 (360m), 9 (400m), 10	Sampling				
For every height	(440m)	rate [Hz.]	Unit			
Line of sight	T6_WI_Dxx_los	1	[-]			
Horizontal wind speed	T6_WI_Dxx_ws	1	m/s			
Wind direction	T6_WI_Dxx_wd	1	0			
Radial wind speed	T6_WI_Dxx_rws	1	m/s			
Radial wind speed deviation	T6_WI_Dxx_rws_dev	1	m/s			
Carrier to noise ratio	T6_WI_Dxx_cnr	1	dB			
Radial wind speed status	T6_WI_Dxx_rws_st	1	[-]			
Overrun Status	T6_WI_Dxx_overrun_st	1	[-]			
Horizontal wind speed status	T6_WI_Dxx_ws_st	1	[-]			
Time	T6_WI_Dxx_TIME	1	ms			

Table 2 Hub height measured signals - MM

Hub height measured signals meteorological mast						
Description	Short name	Sampling rate [Hz.]	Unit			
Wind speed, 120deg boom	MM3_WS80_120	4	m/s			
Wind speed, 240deg boom	MM3_WS80_240	4	m/s			
Sonic wind speed, u component	MM3_S80N_U		m/s			
Sonic wind speed, v component	MM3_S80N_V	4	m/s			
Sonic wind speed, w component	MM3_S80N_W	4	m/s			
Sonic wind speed, status	MM3_S80N_St	[-]				
Air temp	MM3_Tair80	4	°C			
Humidity	MM3_RH80	4	%			
Air pressure	MM3_Pair80	4	hPa			
Wind direction, 120deg boom	MM3_WD80_120	4	0			
Wind direction, 240deg boom	MM3_WD80_240	4	0			

Column Title	Unit	Description
Timestamp (s)		Coordinated Universal Time (UTC)
Distance	(m)	Distance along symmetry axis of lines of sight.
Line of sight	(a.u.)	2 lines of sight possible (0/1)
HWS	(m/s)	Horizontal wind speed
Direction	(°)	Direction of wind
RWS	(m/s)	Radial wind speed
RWSD	(m/s)	Radial wind speed deviation
CNR	(dB)	Carrier to noise ratio
Tilt	(°)	Tilt of system telescopes
Roll	(°)	Roll of system telescopes
RWS status	(a.u.)	0 = RWS is not valid
		1 = RWS is valid
RWS RT status	(a.u.)	0 = no valid RWS within "real time availability period"
		1 = at least 1 valid RWS within "real time availability period"
Overrun Status	(a.u.)	0 = the measurement is late
		1 = the measurement is in time
HWS status	(a.u.)	0 = HWS is not valid
		1 = HWS is valid
HWS RT status	(a.u.)	0 = no valid HWS within REAL TIME AVAILABILITY PERIOD
1	l	1 = at least 1 valid HWS within REAL TIME AVAILABILITY PERIOD

Table 3 WindIris lidar output description

#### 3.2 Wind field reconstruction

As the limitation of a single lidar to distinguish horizontal wind shear and wind direction at the same time (cyclops dilemma), the wind flow is assumed as homogeneous on horizontal plane without wind shear. The WindIris lidar measures consecutively radial wind speeds on its two lines of sight (LOS) and reconstructs HWS and direction based on these two consecutive radial wind speed measurements. Remembering that the wind has three components with respect to three directions, there are now two equations and three unknowns. In order to solve the equations, the vertical wind component of wind is assumed null.

The wind filed reconstruction is illustrated as in Figure 2.  $v_{LOS}$  is the measured LOS radial wind speed. u,v are the wind speed component on horizontal X and Y direction respectively.  $u_h$  is the calculated HWS and  $\gamma$  is the calculated wind direction. This reconstruction is performed on the 10-minute average values of the radial wind speeds, as reconstructing on instantaneous values tends to skew HWS results, as shown later in the report. Finally, individual beam TI is calculated as the standard deviation of the radial wind speed divided by the average over ten minutes. For the wind field, the TI is the average between the individual beam TI's.

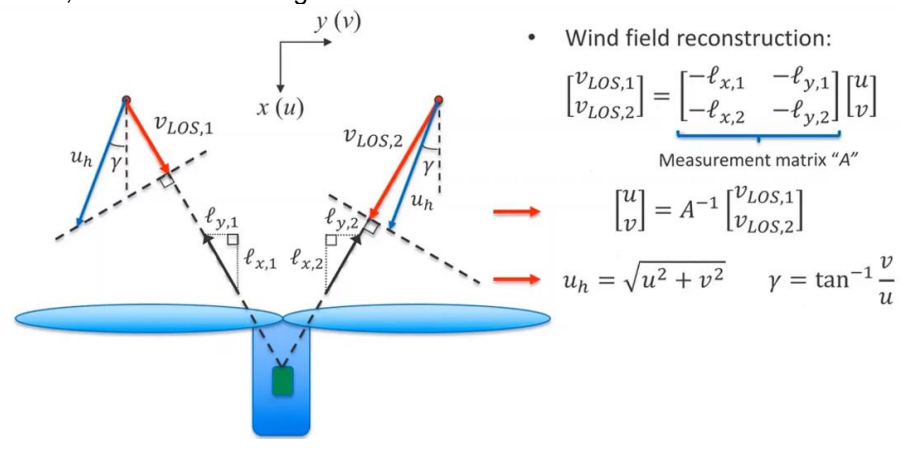


Figure 2: Wind field reconstruction [7]

Considering the measured LOS radial speeds in space and time are variables, a GP is fitted to them. Then velocities at any space and time can be predicted [4] and a 2D (based on a 2-beams lidar) wind field can be reconstructed.

## 3.3 GP implementation

Data between the turbine, met mast, and lidar were combined and synchronized, to provide a robust analysis, and the GP's were successfully applied to this dataset.

The GP implementation pipeline:

- For every 60 seconds of data, fit a GP's hyper-parameters to the provided times, locations, and radial wind speed data. These are considered training GP1's
- 2. Use a second GP layer to smoothen the hyper-parameters from the training GP1's. These are considered the GP2.
- 3. Using the GP2, predict hyper-parameters for individual 30-second, overlapping GP1's at the requested times/locations. These are considered prediction GP1's
- 4. Finally, using these parameters, generate radial wind speed predictions from each prediction GP1, obtaining the requested radial wind field

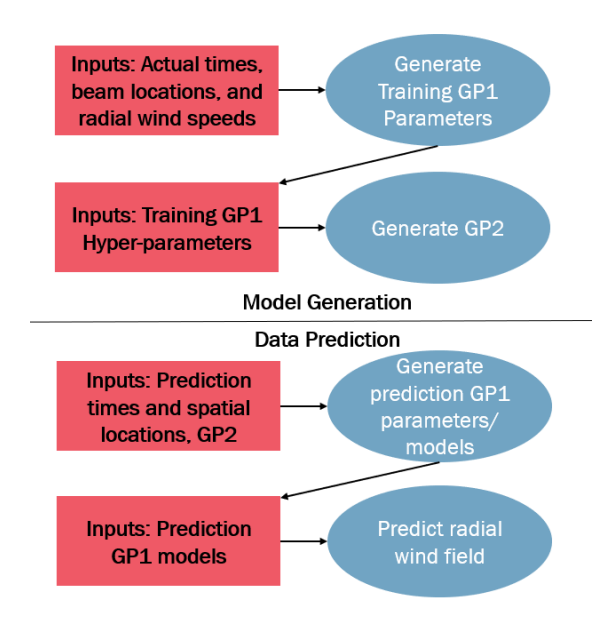


Figure 3: GP implementation pipeline

#### 3.4 Results

#### 3.4.1 Initialization of the GP's

Figure 4 and Figure 5 below show the outputs of the GP process. The first figure shows 60 seconds of LOS radial wind speeds utilizing a training GP1 to predict at one lidar beam location. This is prior to having smoothened hyper-parameters from a GP2. It can be seen that the GP is able to up-sample the lidar measurements of a single beam accurately, following the overall trends of the measurement equipment. Figure 5 on the other hand shows the output at two beam locations for the overall process: utilizing training GP1's, overarching GP2's, and prediction GP1's. Here, upsampling was done in order to provide a lidar prediction for each beam at every

second, unlike the lidar which has staggered measurements (the left and right beams are measured at different times). Once again, a strong correlation between the measurements and the predictions can be seen, validating the ability of the GP's to predict lidar measurements at the beam locations.

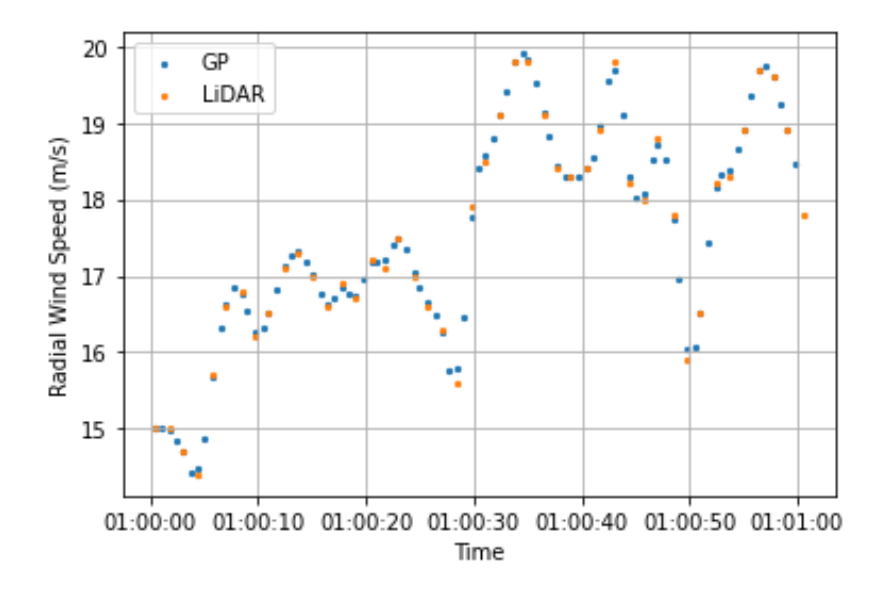


Figure 4: Comparison between lidar output and GP1 prediction at 120m. GP output is upsampled from 0.75 Hz/beam to 1.5 Hz/beam

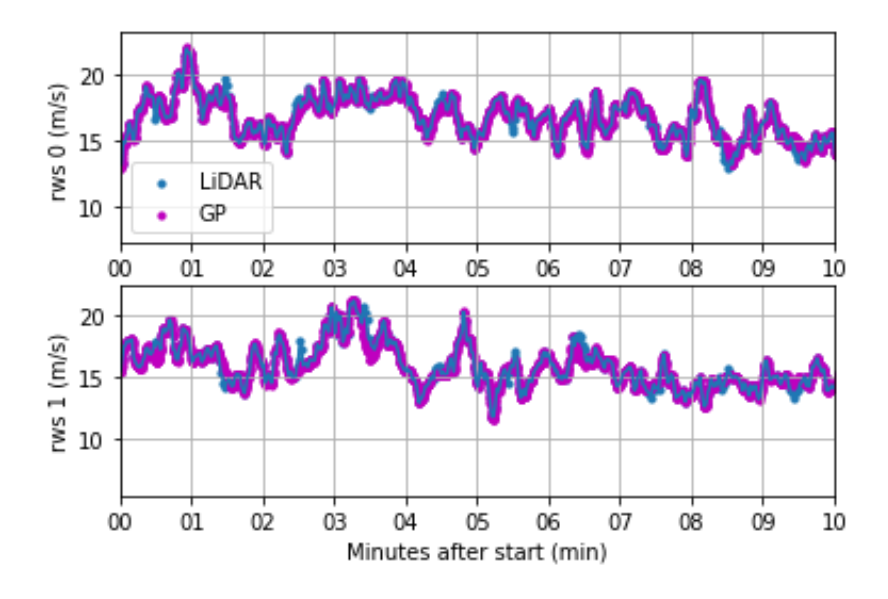


Figure 5: Comparison between lidar output and GP2 prediction at 200m. GP output is up-sampled from a staggered 1.5Hz to a consistent 2Hz

### 3.4.2 Upsampling: 1.5Hz to 4Hz

The first experiment performed on the GP predictions was to see the effect of increasing the data frequency, from 1.5 Hz from the lidar to a total of 8 Hz with the GPs, 4 Hz per beam. This is illustrated in Figure 6 below, which shows a zoomed in view of the radial wind speed predictions and Windlris outputs.

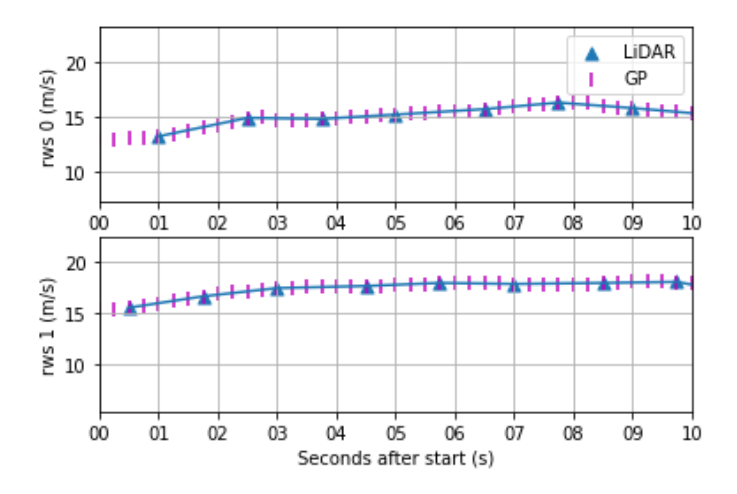


Figure 6: Comparison between lidar output and GP2 prediction at 200m. GP output is up-sampled from a staggered 1.5Hz to a consistent 4Hz

Figure 7 shows the 10-minute wind statistics obtained for this dataset, utilizing the reconstruction methodology for lidar data detailed in the instrumentation report [6]. The values are computed at the meteorological mast distance, 200 m, and this remains consistent for the remainder of the analyses in this report. Here, the 10-minute average values of the lidar data are calculated, and then these are used for reconstruction (vector reconstruction). Note that the dashed line here, and in all future plots with a dashed line, is simply a visualization of a perfect 1-to-1 correlation; if the lidar or GP results were to perfectly match the meteorological mast measurements, then the points would fall on this line.

The HWS appears to be broadly unaffected, and both datasets follow the values output by the met mast. This shows that the GP's have little effect on the HWS output and can predict this well, even at higher frequencies. The TI values do follow those from the met mast, but much less accurately. Additionally, the GP's show a drop in measured TI compared to the lidar values. This is attributed to the inherent properties of the GP's themselves: when lacking measurement data for the regression, they tend towards the mean. As such, when providing 'new' data, they act as a low-pass filter, reducing the standard deviation of the prediction and, therefore, the TI.

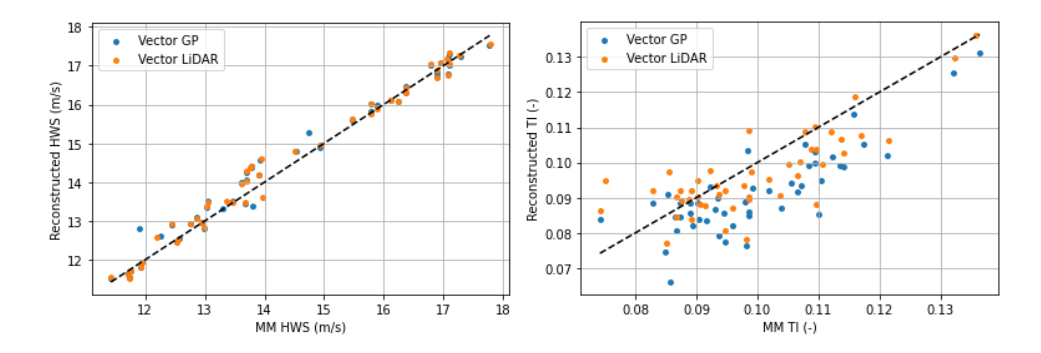


Figure 7: Vector reconstructed HWS (left) and TI (right) for the 1.5Hz lidar and the 8 Hz GP predictions, compared to the MM values. Dashed 1-to-1 lines are provided in order to illustrate differences from the mast data

Note that if reconstruction is undergone with the high frequency data and a 10-minute average is performed afterwards (called a scalar reconstruction), over-speeding is

seen as expected. This occurs with certain lidar configurations, such as two-beam nacelle lidars. The GP's were unable to resolve the over-speeding, as seen in Figure 8. It is possible that the higher data frequency and ability to predict anywhere within the measurement volume may allow GP's to correct for this phenomenon, if different reconstruction methods were used.

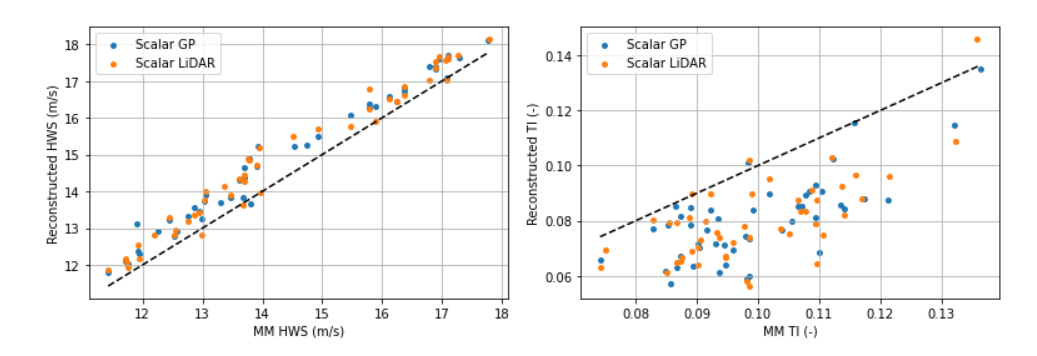


Figure 8: Scalar reconstructed HWS (left) and TI (right) for the 1.5Hz lidar and the 8 Hz GP predictions, compared to the MM values

### 3.4.3 Filling missing data

Next, the ability for the GP to fill missing nacelle lidar data was assessed, with 10 seconds of every minute of every measurement distance range was removed from the data provided to train the GP's. Here, the data was predicted at a frequency of 2 Hz, 1 Hz per beam, as shown in Figure 9. The GP predictions here, where data is missing, drift following the overall trends and the mean, but do not capture the subtle changes in the data.

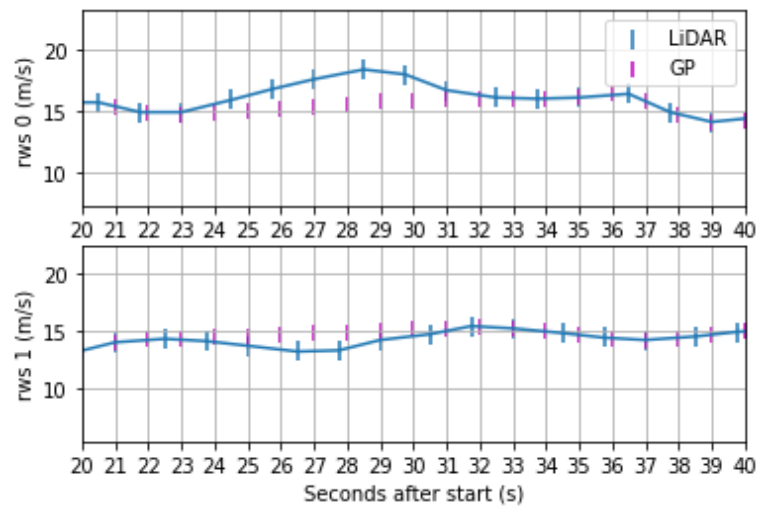


Figure 9: Comparison between lidar output and GP2 prediction at 200m, with 10 second gaps in prediction data at all ranges every minute. GP output is up-sampled from a staggered 1.5Hz to a consistent 2Hz

Figure 10 shows the reconstructed statistics compared to the MM values while the GP's were filling data. Similar to the up-sampling case, the GP's are required to fill data, which tends towards the mean. As such, the average HWS is unaffected, while a drop in the TI is noted.

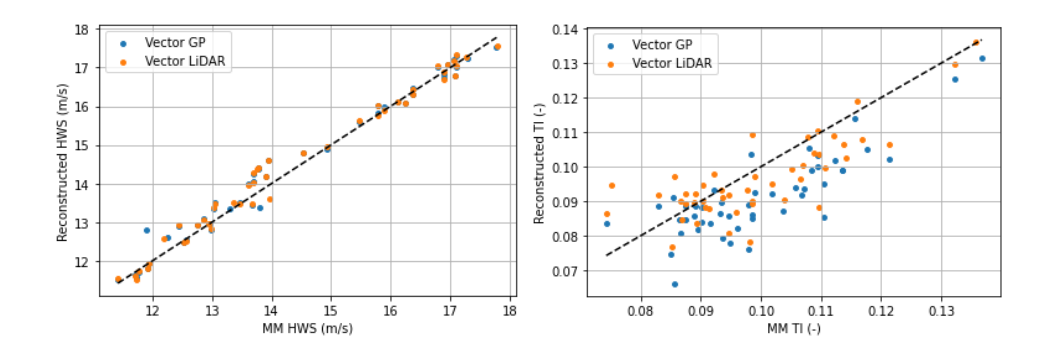


Figure 10: Vector reconstructed HWS (left) and TI (right) for the 1.5Hz lidar and the 2 Hz GP predictions, compared to the MM values, with only 50 seconds of every minute for all ranges provided to the GP model

It is important to note the benefit of including other variables in space when utilizing the GP's. As such, the previous experiment was conducted a second time, however instead of removing ten seconds of data from all ranges, only data from the 200m range was removed. This allows the GP's to predict what is occurring during missing data periods utilizing not just temporal relationships, but also spatial relationships from the information at the other ranges.

Figure 11 shows the same reconstructed statistics for this case. HWS is unaffected, still containing a high correlation. There is a slight improvement compared to the all-ranges-excluded case: the average difference in TI compared to a lidar with 100% data availability decreases from 0.004 to 0.003. This shows the strength of including more physical measurement points when utilizing the GP's, further indicating the need for testing with a lidar whose beams encompass a volume instead of a plane. These configurations naturally have more beams, and allow for more spatial relationships to be generated by the GP's during prediction.

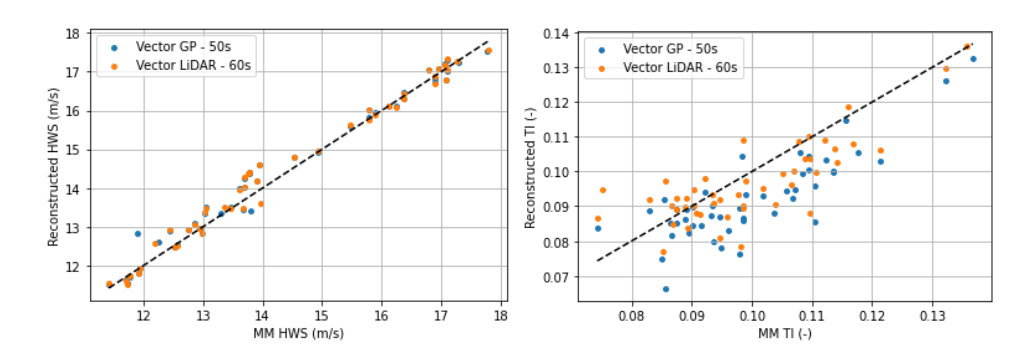


Figure 11: Vector reconstructed HWS (left) and TI (right) for the 1.5Hz lidar and the 2 Hz GP predictions, compared to the MM values, with only 50 seconds of every minute for one range provided to the GP model

#### 3.4.4 Predictions in space

Moving away from time, the GP's can also be used to predict in a region in space outside the locations of the lidar beams. This can be used for a variety of methods/applications, such as that employed in [4] to visualize a horizontal wind field using a "mixture of experts" approach.

Figure 12 shows the predictions of mean radial wind speed in a 2D plane near the lidar measurement height, while Figure 13 shows the uncertainty in the prediction as output by the GP. The mean predicted wind field is visualized, showing turbulent pockets of different length scales. The standard deviation provides a method of assessing GP accuracy at different points in space. It can be directly seen that the uncertainty of the predicted wind speed is much better near the lidar measurement points. Both towards the center and outside the measurement plane, the values approach the mean and the standard deviations get quite high. It is believed that this is due to the design of the GP's: they were created to estimate with points that create a 3D control volume in space. With only two beams, the best that the WindIris can create is a 2D plane for the GP's, limiting accuracy.

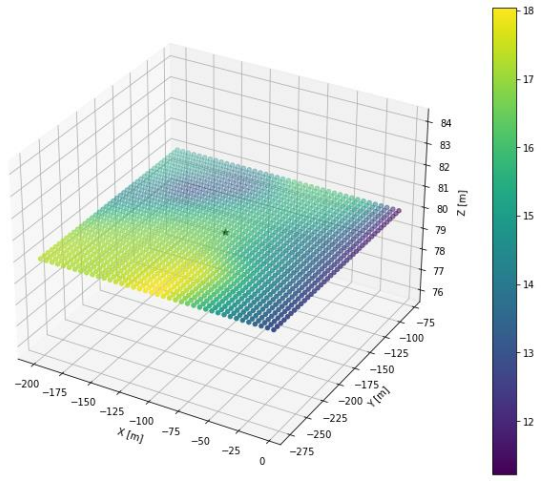


Figure 12: Radial wind speed predictions for one time within a plane using the GP methods.

Colour is the measured radial speed, in m/s, while the star indicates the position of the met mast

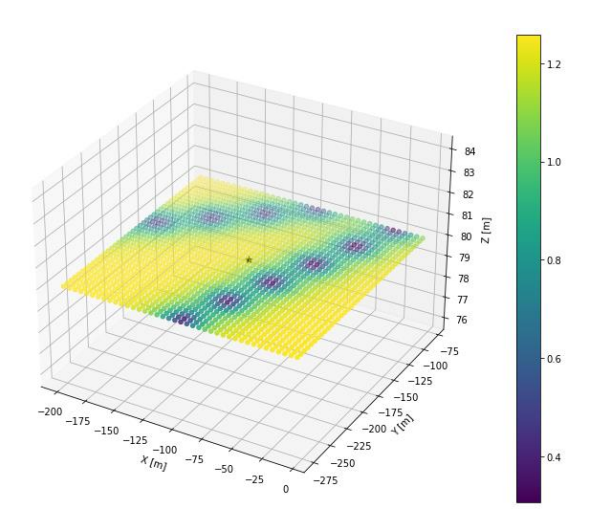


Figure 13: Standard deviation of the GP prediction of radial wind speed for one time within a plane using the GP methods. Color is the measured radial speed standard deviation, in m/s, while the star indicates the position of the met mast

## 3.4.5 Predict in the center of the beams

The GP's can be used to predict the wind speed at the center between the two beams, allowing for an approximation of the HWS. This requires assumptions that the lidar is

not tilting, and that the turbine is facing directly into the wind. However, for the purposes of this report, these can be assumed to be true in order to see how a prediction in space with the WindIris data and how the GP's performs.

Figure 14 shows the results of this methodology, displaying the GP predictions of the 10-minute average wind speed and the TI with the assumptions that the turbine was facing the wind and that the lidar was horizontal. It can be seen that, once again, the 10 minute average mean wind speeds still match those of the MM values, though they are slightly more variable. The TI, on the other hand, shows a large drop overall, indicating that the standard deviation of the data has dropped sharply. This can be seen with a quick comparison of the mean wind speeds in time, shown in Figure 15 for a 10-minute period.

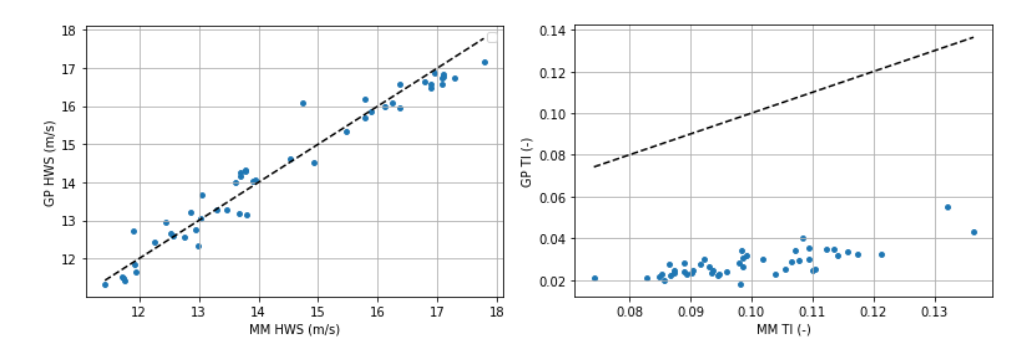


Figure 14: Vector reconstructed HWS (left) and TI (right) for the 2 Hz GP predictions, compared to the MM values, predicting at the center of the lidar beams

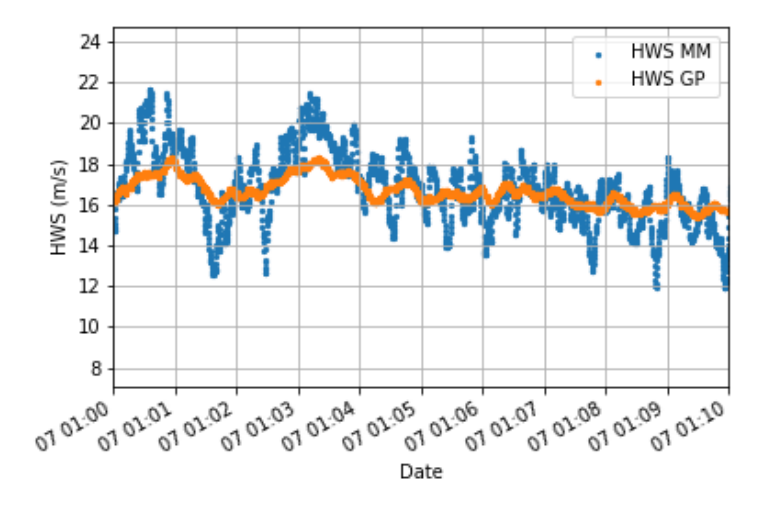


Figure 15: GP prediction of mean HWS between the two lidar beams over 10 minutes, compared to the MM values

## 4 Conclusions

The goal of this project is to explore the potentials of using GP to improve the TI calculation for lidar wind measurements. Several different GP implementations have been tested: up-sampling the data to higher frequency, filling missing data, predicting in space and predicting in the center of the beams. Although GP does not show effective improvements for calculating TI with the data from a two-beam lidar, it does demonstrate that GP can be applied to almost any lidar system to predict LOS radial wind speeds in space and time.

We identified the following recommendations for further exploring the application of GP to improve lidar TI calculation:

- using lidar with more beams for predictions within a volume as opposed to a plane,
- further research into different methods of modelling/calculating TI, and
- deeper investigation into the GP mechanics: change in GP time lengths or overlapping GP1's.

## 5 References

- [1]. A. Sathe and J. Mann, 'A review of turbulence measurements using ground-based wind lidars', Atmos. Meas. Tech., 6, 3147–3167, 2013
- [2]. IEC 61400-12-1:2017, 'Wind power generation systems Part 12-1: Power performance measurements of electricity producing wind turbines'.
- [3]. K.Boorsma, et al, ECN-E-16-044, 'lidar application for wind energy efficiency', 2016
- [4]. C. Stock-Williams et al, 'Wind filed reconstruction from lidar measurements at high-frequency using machine learning', J. Phys.: Conf. Ser. 1102 012003, 2018
- [5]. J.W. Wagenaar, et al, 'Turbine performance validation; the application of nacelle LiDAR', EWEA 2014
- [6]. G. Bergman, J.W. Wagenaar and K. Boorsma, ECN-X-14-085, 'LAWINE instrumentation report', Rev. 2, 2016
- [7]. E. Simley, A. Scholbrock, 'Nacelle Mounted lidar for Wind Energy Applications', Wind Workforce Development Webinar Series, NREL, 2020